



HAL
open science

A detailed in-vitro study of Retinal pigment epithelium's growth as seen from the perspective of impedance spectroscopy analysis

Jocelyn Boutzen, Manon Valet, Agathe Alviset, Valérie Fradot, Lionel Rousseau, Serge Picaud, Gaelle Bazin Lissorgues, Olivier Français

► To cite this version:

Jocelyn Boutzen, Manon Valet, Agathe Alviset, Valérie Fradot, Lionel Rousseau, et al.. A detailed in-vitro study of Retinal pigment epithelium's growth as seen from the perspective of impedance spectroscopy analysis. *Biosensors and Bioelectronics*, 2020, 167, pp.112469. 10.1016/j.bios.2020.112469 . hal-02978002

HAL Id: hal-02978002

<https://hal.science/hal-02978002>

Submitted on 30 Aug 2022

HAL is a multi-disciplinary open access archive for the deposit and dissemination of scientific research documents, whether they are published or not. The documents may come from teaching and research institutions in France or abroad, or from public or private research centers.

L'archive ouverte pluridisciplinaire **HAL**, est destinée au dépôt et à la diffusion de documents scientifiques de niveau recherche, publiés ou non, émanant des établissements d'enseignement et de recherche français ou étrangers, des laboratoires publics ou privés.



Distributed under a Creative Commons Attribution - NonCommercial 4.0 International License

A detailed in-vitro study of Retinal pigment epithelium's growth as seen from the perspective of impedance spectroscopy analysis.

In this paper, we present a method to assess growth and maturation phases of the Retinal Pigment Epithelium (RPE) in-vitro at the cell layer level using impedance spectroscopy measurements on platinum electrodes. We extracted relevant parameters from an electrical circuit model fitted with the measured spectra. Based on microscopic imaging, the growth state of an independent culture developing in the same conditions is used as reference. We show that the confluence point is identified from a graphical analysis of the spectra transition as well as by observing a reconstructed parameter representing the average capacitance of the cell layer. More generally, this work presents a detailed investigation on how cell culture's state relates with either model parameter analysis or with graphical analysis of the measured spectra over a wide frequency band. While applied to the RPE, this work is also suitable for the study of any kind of monolayer epithelial cells growth.

Keywords: Impedance spectroscopy, Retinal Pigment Epithelium, Confluence, Constant Phase Element

1. Introduction

Retinal Pigment Epithelium (RPE) fulfills several support functions such as phagocytosis of aged photoreceptor tips or transport of nutriment and gases to the photoreceptor layer. It also absorbs backscattered light passing through the neuro-retina [1], [2], [3], [4]. Because of its major role, it is of fundamental importance in the eye's physiology that this layer remains unharmed. A damaged RPE is often associated with vision impairing diseases such as in birth acquired diseases like the Leber Congenital Amaurosis or in Age Related Macular Degeneration, a major cause of blindness in the elderly population of western countries [5], [6], [7].

Impedance spectroscopy is a useful tool when used to study a system made of both conductive and dielectric components [8]. The RPE cell layer fulfills both these characteristics because the intracellular medium and extracellular medium (or culture medium) behaves as an electrolyte while the cell's membranes are mainly made of phospholipids that together form an electric insulator [9]. Electrodes are used as bio-interfaces to access the cell layer and therefore to form an electrical circuit. One way to measure the impedance is to apply a sinusoidal voltage variation and to measure the

induced current, or vice versa. If the voltage applied is small enough to consider the system linear (with respect to the standard potential of species in the medium), one can calculate the electrical impedance using $\underline{Z} = \underline{V}/\underline{I}$, where \underline{Z} , \underline{V} and \underline{I} are complex numbers and \underline{Z} is the impedance, \underline{V} the applied voltage, and \underline{I} the measured current [10]. Impedance is measured at several frequencies to construct the electrical impedance spectra (module and phase).

Impedance spectroscopy is used in a wide range of biological applications such as growth monitoring of yeasts [11], food processing [12], or measurement of plated cells micro motion [13].

Assessing growth state of the RPE layer in-vitro can be useful in the context of engineered tissues for grafts purposes [14], [15]. Furthermore, assessing the growth state of a cell layer over a surface as large as several mm² is done in a single impedance spectroscopy measurement. On the other hand covering an equivalent area would require many microscopic images to be taken.

Measurement of the trans-epithelial electric resistance (TEER) has been investigated using similar methods and is used as an indicator of epithelial cell's state in-vitro [16], [17], [18] or in-vivo [19], [20].

In this paper, the uses of different impedance model parameters are presented in order to assess the cell's state of development.

The TEER is linked to the cell layer's tight junctions resistance presented in this paper. It indicates the tightness of the junctions therefore providing a quantitative measurement of the layer's barrier function. Moreover, based on the parameters extracted from the electrical model, a reconstructed capacitance is also presented and linked to the state of development of the cell membranes. Evolutions of the parameters are then associated with graphical evolution of the impedance spectrum as well as with microscopic images of cell state. Altogether, this study presents an innovative investigation of RPE tissue growth through the perspective of impedance spectroscopy.

2. Material and Methods

Impedance measurement ([1Hz, 1MHz] frequency bandwidth; 10 mV_{rms} amplitude; 20 points per frequency decade) was performed on a 1.88 mm diameter planar platinum electrode deposited on a glass substrate and surrounded by a reference electrode with a gap of 100 μm. Platinum is widely used as electrode material and is considered biocompatible [21], [22], [23]. We used a Faraday cage to shield the setup from noise. We considered the voltage applied to be small enough to be able to neglect damages to the

cell layer during the measurement process, either through electrochemical reactions or through direct influence of the applied electric field.

Cells were seeded at an initial concentration of 100.000 cells per chamber in Dulbecco's Modified Eagle Medium (DMEM) with 20 % Fetal Calf Serum (FCS). They developed at the surface of the electrode. Medium has been changed at day 1 to remove the cells that had not attached to the bottom of the device, and at day 9 to refill the chambers.

Except for the initial cellular concentration and for the number of impedance point measured in each spectrum, the experimental impedance measurement setup and cell culture procedures used in this article were identical to what had been previously presented [24]. Nevertheless, setup and culture details are given in the supplementary information section S.1 to S.3 and Supplementary Figure 1 of this article. A noise study of this experimental setup can be found in the supplementary materials of [24].

3. Results and Discussion

3.1. Follow-up using microscopic imaging

The RPE cell layer's evolution can be divided in two phases. The first consists in division of the cells until they cover the area available. Then a maturation phase takes place, with consolidation of tight junctions and cells taking their final shape [25], [26].

Figure 1 shows microscopic images taken at the same location of a culture developing in the same conditions as the one whose impedance is being measured. Images were taken at the date indicated in the timestamp of each pictures, day 0 being the seeding day. At day 1 and 2, the cell layer was clearly not covering all space available yet. At day 3 the cell layer's density was higher but one cannot identify clear junctions between individual cells. At day 4 the cells delimitations were sharper, indicating that junctions had formed between them. Therefore one can states that confluence was reached between day 3 18h59 and day 4 17h36. This means that cells were covering the entire surface available. However a slight increase in cell density still happens after day 4, with cells getting smaller as seen on the picture taken on day 10. This gives an indication of the time window before achieving confluence, which will be linked to the model's parameter evolution singularities thereafter.

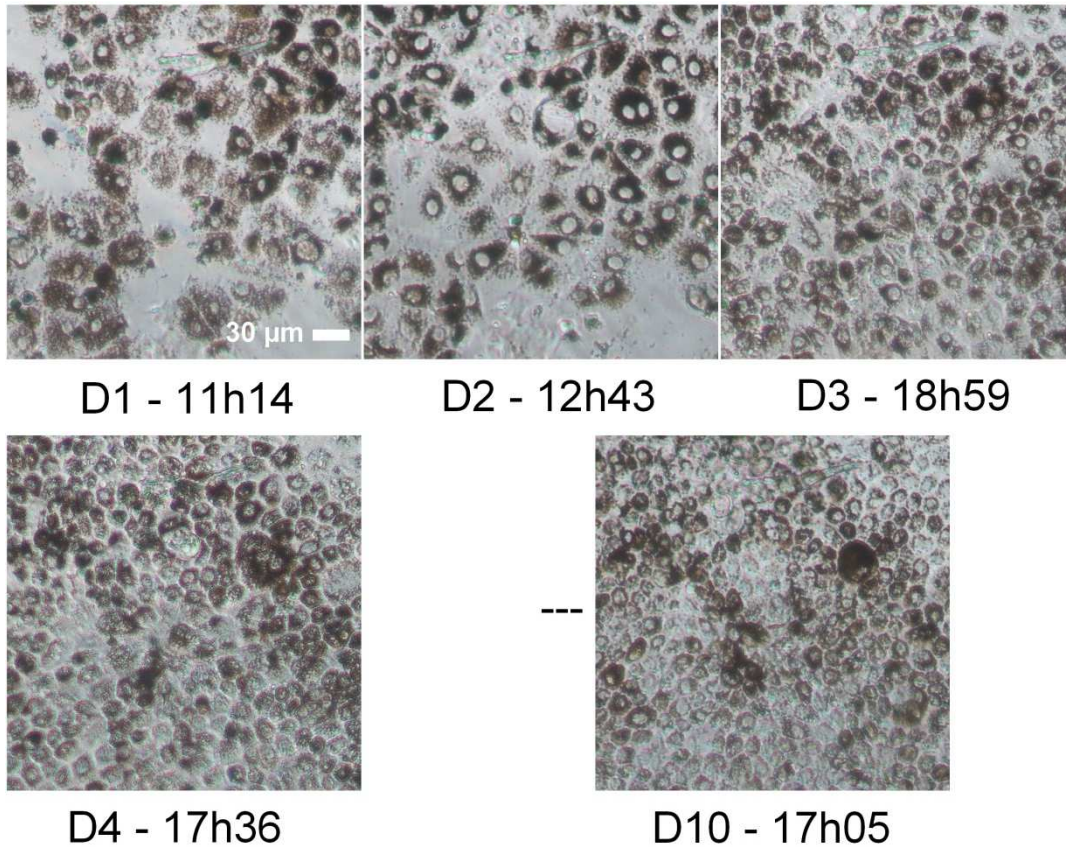


Figure 1 Cell culture evolution in a platinum free region next to the disk electrode, assessed by microscopic images. Images indicate that confluence happens between Day 3 (18h59) and Day 4 (17h36). The cell culture presented here is not the one measured by impedance spectroscopy and presented in Figure 3 to prevent repetitive manipulation of the latter. However, it is cultured using exactly the same procedure and environment. Scale bar applies to all pictures.

3.2. The electrical circuit model

A simplified electrical circuit model was linked with the impedance measurements. We previously presented this model in [24] where we evaluated independence between the extracted parameters.

A short description of the model is presented thereafter. Details about the model establishment and simplifications are given in the supplementary information section S.4 and Supplementary Figure 2 of this article for an easier reading. Some parts of the figures represented there are similar to what has been presented in [24] because we used the same electrical model and experimental setup for a different application in the present article.

Two constant phase elements (CPE) were associated with the electrode-electrolyte interface $CPE_{el} (Q_{el}, \alpha_{el})$ as well as with the cell layer $CPE_{cell} (Q_{cell}, \alpha_{cell})$. R_{cell} resistance

was associated with free space between cells. R_{med} resistance represented the culture medium path. The schematic of the model is given in Figure 2 A and its impedance is then equation (1):

$$\underline{Z}(\omega) = \frac{1}{Q_{el}(j\omega)^{\alpha_{el}}} + \frac{R_{cell}}{1 + R_{cell}Q_{cell}(j\omega)^{\alpha_{cell}}} + R_{med} \quad (1)$$

Parameters of the model were extracted using least-square fitting of the model to the data and done using Levenberg-Marquardt algorithm from the spectrometer software. Monitoring of cells related parameters with time are shown Figure 2 without any treatment nor filtering. They highlight some specific steps of the cell growth. Figure 3 gives the evolution of the impedance spectrum from which the parameters are extracted. An illustration of the quality of the fit (continuous line) with respect to the data (markers) using the spectrum measured day 4, 8h22 is given Figure 3 C.

For frequencies above 100 Hz, one can only consider the cell and culture medium related parts. It is then possible to calculate an effective capacitance from the parameters of the electrical circuit model. This capacitance accounts for the mean capacitance of the cell layer. It has several definitions depending on the geometric distribution of the time constants at the origin of the CPE behavior [27], [28]. In the case of our experiment, a surface distribution of time constant was present. The effective capacitance definition C_{eff} for such a distribution is given in [29] and written as follows, equation (2):

$$C_{eff} = Q_{cell}^{\frac{1}{\alpha_{cell}}} (R_{med}^{-1} + R_{cell}^{-1})^{\frac{\alpha_{cell}-1}{\alpha_{cell}}} \quad (2)$$

3.3. Evolution of the model's parameters during growth

While the cell layer was taking shape, the parameters of the electrical circuit model as well as the reconstructed capacitance were observed as seen on Figure 2. Maxima are present in the evolution of parameters $1/Q_{cell}$ and $1/C_{eff}$ at day 6 and day 4 respectively. $1/C_{eff}$ parameter reaches its maximum on day 4, 8h22 as shown with a black line Figure 2 C. This date was also associated with the $1/Q_{cell}$ inflexion point as shown Figure 2 B. To determine the inflexion point we calculated the differential of $f = 1/Q_{cell}$ such as

$diff(f(n)) = f(n + 1) - f(n)$. The differential is shown in the inset Figure 2 B. At day 4 8h22 R_{cell} is not reaching any singular value (Figure 2 A). This date was associated with a graphical transition in the spectra (Figure 3). Both $1/Q_{cell}$ and $1/C_{eff}$ parameters values stabilized after day 10. Regarding parameter R_{cell} , its evolution was more erratic but tended to stabilize around day 12. This parameter was also sensitive to perturbations of the medium, such as temperature and possible slight pH variations happening when the culture medium is changed or when the culture is observed under the microscope outside the CO₂ rich environment of the incubator. Following these events, and during the beginning of the culture, the R_{cell} parameter settled back then increased. Interestingly, these perturbations were barely noticeable on $1/Q_{cell}$ and $1/C_{eff}$ parameters. Finally, the evolution of α_{cell} was close to monotonic with a maximum almost invisible. The parameters presented (Figure 2) have to be associated with the spectra (Figure 3). The impedance of 3 simultaneous cell cultures has also been recorded in order to provide statistical information on the evolution of the parameters (Supplementary Figure 3 of the supplementary information section). Distribution of the maximum's date of $1/C_{eff}$ had a mean value of 4 days and 17 hours with a standard deviation of 10 hours 49 minutes.

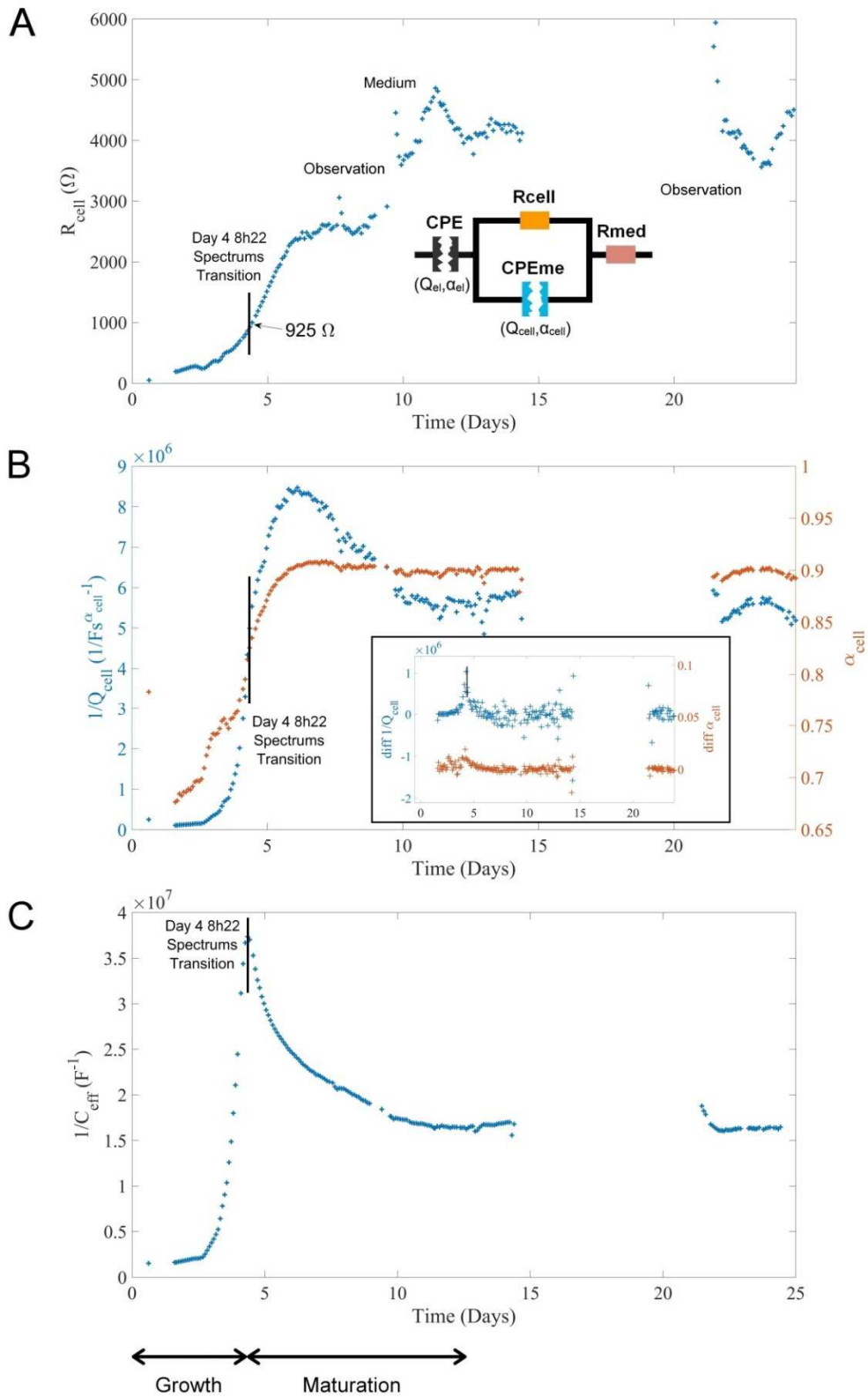


Figure 2 Evolution of the electrical model parameters after cell seeding. Parameters are extracted from the spectra presented Figure 3 by least square fitting. A - R_{cell} . B - $1/Q_{cell}$ (blue) and α_{cell} (red). The inset in B shows the differential of both parameter in order to identify the inflexion point. C - $1/C_{eff}$, where C_{eff} is the capacitance reconstructed from the model parameters. The electrical circuit in A is the model associated with the electrode and cell layer.

3.4. Graphical analysis of the spectra measured

Parameters of the model were extracted from the impedance spectra (Figure 3). Two phases have been identified when looking at the graphical shape evolution of those spectra. At the beginning of the measurement (spectrum label “D0” on Figure 3 A) cells were not yet visible on the measurements and a direct transition from CPE behavior (charge storage associated with the electrode-electrolyte interface) to resistive behavior (culture medium) was observed. When the cells started to multiply, other transitions appeared. They are related to the formation of dielectric cellular membranes therefore adding a new relaxation frequency in the system. A transition can be seen between CPE behavior of the electrode-electrolyte interface and resistive behavior of the reducing space in between the cells. For a high enough frequency (above 4 kHz in our case), a CPE behavior associated with cell’s membranes was measured. Transition to a culture medium related resistive behavior for the highest frequencies measured (above 100 kHz) was then observed, as in a situation without cells.

As shown with dashed arrows (Figure 3 A), the resistive behavior (shifting to higher module values) and CPE behavior (shifting to higher frequency and module values) associated with cell’s development were evolving without singularities.

However this is only true up to day 4. A transition spectrum indeed appeared. It is shown with dot markers on Figure 3 A and B. After this transition spectrum (Figure 3 B) one can observe that the cell’s CPE behavior is not shifting to higher module and frequency values but to lower module and frequency values, as shown with dashed arrows (Figure 3 B).

The resistive behavior keeps shifting toward higher module values. The transition spectrum appeared at day 4, 8h22. This date matches the time when reconstructed parameter $1/C_{eff}$ reached its maximum.

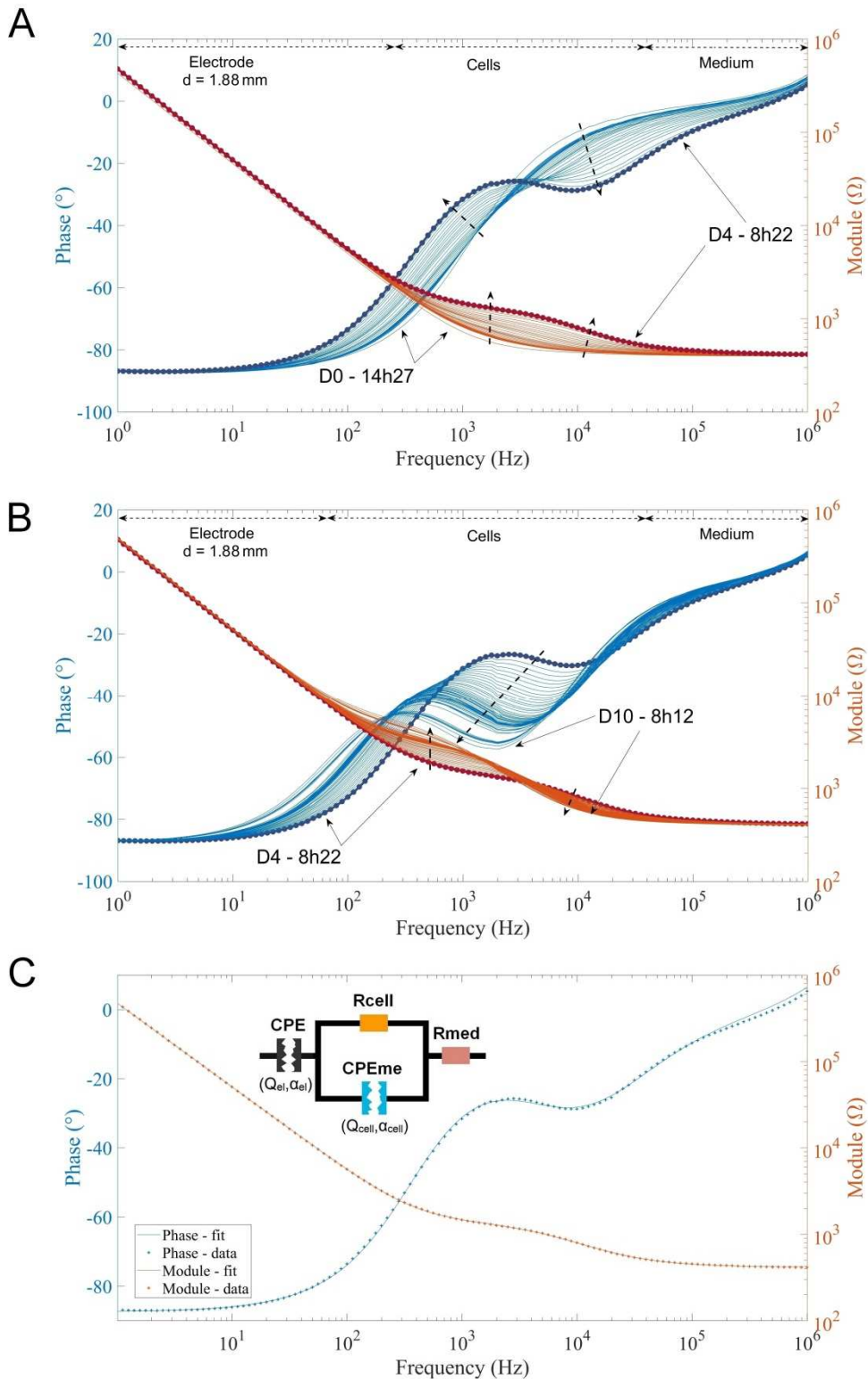


Figure 3 A - Measured spectra (module in red and phase in blue) between Day 0 and Day 4, associated with the culture growth phase. B - Measured spectra between Day 4 and Day 10, associated with the culture maturation phase. The transition spectrum measured on Day 4 at 8h22 is shown with thick lines and round shape markers on A and B. Dashed arrows indicate spectrum evolution with time. C – Illustration of the quality of the fit. The data (+) shows the spectrum measured at day 4 8h22 (shown with dot markers on A and B). The continuous line is the associated fit. The electrical circuit is the model associated with the electrode and cell layer.

3.5. Discussion

In this work the RPE's cells development was studied based on impedance analysis as well as with imaging of cell growth. The different phases of its development have been investigated, namely the growth phase before confluence, and the maturation phase that follows. Firstly, a cell culture follow-up has been performed using microscopic imaging. We have then been able to conclude that in the conditions of our experiments, confluence of the cell layer occurs between end of day 3 and end of day 4 of the cell culture. However microscopic imaging involves manipulation of the culture. Also removing them from the incubator environment affects temperature and stress condition of the cells. It could also lead to cell culture contamination. Therefore one goal of this study was to provide an alternative mean to identify the confluence point using impedance spectroscopy, a live non-invasive technic allowing non-destructive measurements of the cell layer inside the incubator's environment. Parameters extracted from an electrical circuit model are used as quantitative indicators of the layer's state. Details about independence of those parameters are given in a previous study involving the same model and experimental setup [24]. Several singularities were identified within the evolution of the observed parameters, such as the maxima of $1/Q_{cell}$ and $1/C_{eff}$, or R_{cell} and α_{cell} stabilization. However several converging information were obtained and used to discriminate between those singularities. Microscopic imaging showed that confluence of the cell layer happened between the ends of day 3 and 4. The parameter $1/C_{eff}$ presented a maximum, whose date was measured to have a mean value of 4 days 17 hours with a standard deviation of 10 hours 49 minutes. Finally, given that other parameter's singularities did not match the time window of confluence as determined by microscopic imaging, we state that the confluence point is reached when $1/C_{eff}$ reached its maximum. C_{eff} can be associated with the mean capacitance of the cell layer, a physical characteristic originating from cellular membranes. It is not surprising that the reconstructed C_{eff} parameter's singularity can be associated with confluence point since confluence coincides with cell membranes covering the electrode. After confluence, cells are mostly forming junctions and are changing shape [26], [30], which accounts for the effective capacitance change seen after day 4 (Figure 2 C). On the other hand R_{cell} , associated with the resistance of cellular junctions (or of free space between cells before confluence), have not reached a maximum at all. Indeed at day 4 8h22, R_{cell} value is 925 Ω , far below the level reached after day 12, of about 4000 Ω . It is therefore clear that at confluence, the cell layer is far from being a barrier to electrolytes yet. α_{cell} is

considered to represent the spatial distribution of cell's phospholipids dipolar moments because they are the fundamental building blocks at the origin of the cell layer's capacitance. They are also molecular size elements, which can be put in relation, size wise, with what has been presented in [25] in the case of the electrode surface. When the cell layer is growing, cell size and shape are homogenizing which reflects on the α_{cell} parameter increasing. Yet it is not at its maximum at the time of confluence. Indeed before confluence the cell layer is becoming more and more homogenous but cells are not yet tied to each other by their side. Cells junctions are starting to build up after confluence, therefore rearranging the cell membranes. This changes the phospholipids orientation to a more organized and definitive state. The consolidation of cellular junction through formation of more actin filaments between cells then continues. By monitoring the R_{cell} value, the progressive junction building can then be analyzed, like this is done with TEER monitoring.

Geometric observation of the spectra's shape and evolution can also provide a lot of information on tissue's state of development. As depicted in the result section, a modification of the spectra shift occurs when confluence is reached. Applying this principle in a quantitative way consists in plotting the impedance value at a determined frequency versus time, for example 5 kHz, similarly to what was done in [30]. Cell membrane's CPE frequency region is therefore targeted. Using a lower frequency (for example 800 Hz) it is possible to target cells junctions, giving direct information on the TEER when the high frequency culture medium resistance value is subtracted. However, spectra shift, as seen Figure 3 A and B can interfere with a fixed frequency choice. Therefore, if detailed information about the layer, or discrimination between membranes state and junctions state are needed, a parameter extraction procedure such as the one presented in this article can be used.

4. Conclusion

Confluence is a well-known crossover point in single layer epithelial cell cultures. In this work a detailed alternative approach is highlighted and put into perspective with the microscopic evaluation of RPE state of development. Using our impedance spectroscopy experimental setup, measurements were performed in a repetitive manner inside the incubator's environment and without the use of any chemical markers that could alter the cell's state. Moreover, this evaluation was done using a millimeter size electrode, covering in one measurement an area larger than one could cover with a single picture taken through the microscope. From those measurements, it was possible to determine in an automated way the confluence point of the layer. This was done by locating $1/C_{eff}$'s

maximum, where C_{eff} is a parameter reconstructed from fitted parameters of the electrical circuit model and considered to represent the mean capacitance of the cell layer. Furthermore, and while we have shown that R_{cell} doesn't reach a specific point at confluence, this parameter, also known as Trans-Epithelial Electrical Resistance, still gave a useful information on the layer's barrier function. Besides, details were provided on how to analyze the geometric evolution of the spectra measured when cells are growing. It had therefore been possible to quickly identify the confluence point, before analyzing extracted parameters from the model if detailed information about the layer were needed. Such a procedure, based on a large analysis of impedance spectrum properties, can be adapted to many in-vitro cell culture studies, especially on epithelial tissue.

Acknowledgment

Jocelyn Boutzen acknowledges support from Ecole Normale Supérieure Paris-Saclay scholarship. **The authors thank Héléna Boutzen for helpful comments and English proofreading.** This work was supported by French state funds managed by the Agence Nationale de la Recherche within the Investissements d'Avenir program, LABEX LIFESENSES[ANR-10-LABX-65], IHU FOReSIGHT [ANR-18-IAHU-0001]. The authors acknowledge support from ESIEE Paris (Noisy-le-Grand) for clean room fabrication and instrumentation on internal funds.

5. Bibliography

- [1] F. Mazzoni, H. Safa, and S. C. Finnemann, *Exp. Eye Res.*, vol. 126, pp. 51–60, Sep. 2014, doi: 10.1016/j.exer.2014.01.010.
- [2] M. Dubald, S. Bourgeois, V. Andrieu, and H. Fessi, *Pharmaceutics*, vol. 10, no. 1, Art. no. 1, Mar. 2018, doi: 10.3390/pharmaceutics10010010.
- [3] M. Boulton and P. Dayhaw-Barker, *Eye*, vol. 15, no. 3, pp. 384–389, May 2001, doi: 10.1038/eye.2001.141.
- [4] O. Strauss, *Physiol. Rev.*, vol. 85, no. 3, pp. 845–881, Jul. 2005, doi: 10.1152/physrev.00021.2004.
- [5] I. Bhutto and G. Lutty, *Mol. Aspects Med.*, vol. 33, no. 4, pp. 295–317, Aug. 2012, doi: 10.1016/j.mam.2012.04.005.
- [6] J. Feher, I. Kovacs, M. Artico, C. Cavallotti, A. Papale, and C. Balacco Gabrieli, *Neurobiol. Aging*, vol. 27, no. 7, pp. 983–993, Jul. 2006, doi: 10.1016/j.neurobiolaging.2005.05.012.
- [7] H. Morimura, G. A. Fishman, S. A. Grover, A. B. Fulton, E. L. Berson, and T. P. Dryja, *Proc. Natl. Acad. Sci.*, vol. 95, no. 6, pp. 3088–3093, Mar. 1998, doi: 10.1073/pnas.95.6.3088.
- [8] S. Lanfredi and A. C. M. Rodrigues, *J. Appl. Phys.*, vol. 86, no. 4, pp. 2215–2219, Jul. 1999, doi: 10.1063/1.371033.

- [9] D. A. Dean, T. Ramanathan, D. Machado, and R. Sundararajan, *J. Electrostat.*, vol. 66, no. 3–4, pp. 165–177, Mar. 2008, doi: 10.1016/j.elstat.2007.11.005.
- [10] J. R. Macdonald, *Ann. Biomed. Eng.*, vol. 20, no. 3, pp. 289–305, May 1992, doi: 10.1007/BF02368532.
- [11] A. Soley *et al.*, *J. Biotechnol.*, vol. 118, no. 4, pp. 398–405, Sep. 2005, doi: 10.1016/j.jbiotec.2005.05.022.
- [12] Y. Ando, K. Mizutani, and N. Wakatsuki, *J. Food Eng.*, vol. 121, pp. 24–31, Jan. 2014, doi: 10.1016/j.jfoodeng.2013.08.008.
- [13] I. Giaever and C. R. Keese, *Cell Biol.*, p. 5.
- [14] A.-J. F. Carr, M. J. K. Smart, C. M. Ramsden, M. B. Powner, L. da Cruz, and P. J. Coffey, *Trends Neurosci.*, vol. 36, no. 7, pp. 385–395, Jul. 2013, doi: 10.1016/j.tins.2013.03.006.
- [15] N. Onnela, V. Savolainen, K. Juuti-Uusitalo, H. Vaajasaari, H. Skottman, and J. Hyttinen, *Med. Biol. Eng. Comput.*, vol. 50, no. 2, pp. 107–116, Feb. 2012, doi: 10.1007/s11517-011-0850-z.
- [16] B. Srinivasan, A. R. Kolli, M. B. Esch, H. E. Abaci, M. L. Shuler, and J. J. Hickman, *J. Lab. Autom.*, vol. 20, no. 2, pp. 107–126, Apr. 2015, doi: 10.1177/2211068214561025.
- [17] O. Y. F. Henry, R. Villenave, M. J. Cronce, W. D. Leineweber, M. A. Benz, and D. E. Ingber, *Lab. Chip*, vol. 17, no. 13, pp. 2264–2271, 2017, doi: 10.1039/C7LC00155J.
- [18] J. Yeste *et al.*, *Lab. Chip*, vol. 18, no. 1, pp. 95–105, 2018, doi: 10.1039/C7LC00795G.
- [19] M. Uematsu *et al.*, *Ophthalmic Res.*, vol. 39, no. 6, pp. 308–314, 2007, doi: 10.1159/000109986.
- [20] M. Kusano, M. Uematsu, T. Kumagami, H. Sasaki, and T. Kitaoka, *Cornea*, vol. 29, no. 1, pp. 80–85, Jan. 2010, doi: 10.1097/ICO.0b013e3181a3c3e6.
- [21] N. Lago, K. Yoshida, K. P. Koch, and X. Navarro, *IEEE Trans. Biomed. Eng.*, vol. 54, no. 2, pp. 281–290, Feb. 2007, doi: 10.1109/TBME.2006.886617.
- [22] V. Vince, M.-A. Thil, C. Veraart, I. M. Colin, and J. Delbeke, *J. Biomater. Sci. Polym. Ed.*, vol. 15, no. 2, pp. 173–188, Jan. 2004, doi: 10.1163/156856204322793566.
- [23] T. Geninatti *et al.*, *Biomed. Microdevices*, vol. 17, no. 1, p. 24, Feb. 2015, doi: 10.1007/s10544-014-9909-6.
- [24] J. Boutzen *et al.*, *Biosens. Bioelectron.*, 2020, doi: 10.1016/j.bios.2020.112180.
- [25] M. T. Flood, P. Gouras, and H. Kjeldbye, *Invest. Ophthalmol. Vis. Sci.*, vol. 19, no. 11, pp. 1309–1320, Nov. 1980.
- [26] B. Matsumoto, C. J. Guérin, and D. H. Anderson, *Invest. Ophthalmol. Vis. Sci.*, vol. 31, no. 5, pp. 879–889, May 1990.
- [27] G. J. Brug, p. 21, 1984.
- [28] C. H. Hsu and F. Mansfeld, *CORROSION*, vol. 57, no. 9, pp. 747–748, Sep. 2001, doi: 10.5006/1.3280607.
- [29] B. Hirschorn, M. E. Orazem, B. Tribollet, V. Vivier, I. Frateur, and M. Musiani, *Electrochimica Acta*, vol. 55, no. 21, pp. 6218–6227, Aug. 2010, doi: 10.1016/j.electacta.2009.10.065.
- [30] W. Gamal *et al.*, *Biosens. Bioelectron.*, vol. 71, pp. 445–455, Sep. 2015, doi: 10.1016/j.bios.2015.04.079.